Physics Letters A 384 (2020) 126041

Contents lists available at ScienceDirect

Physics Letters A

www.elsevier.com/locate/pla

Enhancement of image quality by using metamaterial inspired energy harvester

Fatih Ozkan Alkurt [a], Olcay Altintas [a], Meliksah Ozakturk [b], Muharrem Karaaslan [a], Oguzhan Akgol [a], Emin Unal [a], Cumali Sabah [c,d,*]

[a] Department of Electrical and Electronics Engineering, Faculty of Engineering and Natural Sciences, Iskenderun Technical University, 31200, Iskenderun, Hatay, Turkey
[b] Department of Energy Systems Engineering, Faculty of Engineering and Natural Sciences, Iskenderun Technical University, 31200, Iskenderun, Hatay, Turkey
[c] Department of Electrical and Electronics Engineering, Middle East Technical University - Northern Cyprus Campus (METU-NCC), Kalkanli, Guzelyurt, 99738, TRNC / Mersin 10, Turkey
[d] Kalkanli Technology Valley (KALTEV), Middle East Technical University - Northern Cyprus Campus (METU-NCC), Kalkanlı, Guzelyurt, 99738, TRNC / Mersin 10, Turkey

ARTICLE INFO

Article history:
Received 1 July 2019
Received in revised form 13 September 2019
Accepted 3 October 2019
Available online 9 October 2019
Communicated by L. Ghivelder

Keywords:
Metamaterial
Energy harvester
Sub-wavelength imaging
Antenna

ABSTRACT

Metamaterial energy harvester based subwavelength imaging structure is presented. Besides, 2×2 array patch antenna is designed to create incident radiated signal towards the proposed harvester structure. Harvested energy is converted to DC voltage signal by using Schottky diodes and each cell is represented by 256 grey levelled pixel value. Therefore, any incident electromagnetic wave placed in the operating frequency range can be monitorized. In the experimental study, experiments are realized with and without antenna to investigate the effects of instantaneous electromagnetic waves and the observed images. Afterwards, another experiment is conducted to observe the effects of metal plate which is located between the antenna and the harvester structure. The last experiment is performed by using a Yagi Uda antenna for sub-wavelength imaging. The proposed harvester structure can be used in various applications such as energy harvesting, incident wave tracing, crack detection, spy device detection, medical imaging, and so on.

© 2019 Elsevier B.V. All rights reserved.

1. Introduction

Metamaterials (MTMs) are artificial materials composed of metallic layers with the dielectric substrates and are not found in nature. First approach about MTM is conducted by Victor Veselago in 1968 and a hypothetical substance having simultaneously negative values of permittivity and permeability is proposed in [1]. After a long time, in 2000, Smith et al. has derived a composite medium with simultaneously negative permittivity and permeability [2]. Moreover, Shelby et al. has supported their study on obtaining negative refraction index with experimental studies in 2001 [3]. In 2004, another study is carried out by Smith et al., they have examined MTMs and negative index of refraction [4]. According to the development of MTM technology, MTMs are designed for various areas such as electromagnetic (EM) wave cloaking [5,6], optical cloaking [7], polarization conversion [8], antenna applications [9,10], super-lensing [11,12], sensing [13–16], absorbers [17–22], energy harvesting [23–30] and imaging [31,32].

Nowadays, MTM based absorber studies have increased to absorb and harvest EM signals at microwave regime. In 2008, Landy et al. has designed, fabricated and analyzed a MTM structure which consists of two separated resonators to absorb incident EM waves [17]. Dincer et al. proposed a perfect MTM absorber based on square resonator with gap configuration for the frequency regimes of GHz and THz [18]. Another study is carried out to obtain dual band perfect absorption with MTM structure [19]. Also, Ta et al. have reported MTM based polarization insensitive dual band absorber for terahertz regime and their study contains design, fabrication and characterization phases [20]. Watts et al. have investigated the flexibility performance of MTM inspired absorbers and discussed the applications of MTM absorber technologies [21]. MTM absorber based multifunctional sensor is suggested by Akgol et al. and their structure can measure the density, humidity and pressure according to absorption characteristics in X band [22]. In addition, polarization insensitive MTM based absorber structure for EM energy harvesting application is examined by Cheng et al.

* Corresponding author at: Department of Electrical and Electronics Engineering, Middle East Technical University - Northern Cyprus Campus (METU-NCC), Kalkanli, Guzelyurt, 99738, TRNC / Mersin 10, Turkey.
E-mail address: sabah@metu.edu.tr (C. Sabah).

https://doi.org/10.1016/j.physleta.2019.126041
0375-9601/© 2019 Elsevier B.V. All rights reserved.

They also explained compatibility of proposed harvester structure to different frequency bands [23]. Devi et al. presented RF energy harvesting applications by using split ring MTM resonators at 1800 MHz [24]. Mulazimoglu et al. proposed a hexagonal shaped EM energy harvester for the frequency regime where EM pollutions are situated [25]. Another study is conducted for energy harvesting by split ring resonators, resistive load is located onto the gap of split ring resonator and the effect of resistance value on absorption is investigated [26]. Nevertheless, Lalj et al. have proposed the polarization insensitive MTM based microwave absorber for EM energy harvesting application by design of rotational symmetric resonator layer [27]. In the study of Duan et al., they presented a MTM energy harvester to convert incident wave to DC current with rectifying functionality [28]. Further, Unal et al. proposed a tuneable MTM based energy harvester and sensor applications; also, they used the golden ratio to determine the dimension parameters [29]. Mulla and Sabah have presented a MTM structure to harvest solar energy and they also investigated their structure for infrared and ultraviolet regime [30]. Karaaslan et al. have proposed multilayered square split ring resonators to harvest microwave energy [31]. Wood et al. have examined subwavelength imaging by using metal dielectric system [32]. In another study, Xie et al. have developed a subwavelength camera for 6.3 GHz by using MTM based absorber structures [33]. Similarly, microwave imaging is achieved by Alkurt et al. with microwave absorber structure [34]. Finally, Yagitani et al. proposed an EBG absorber plane to obtain 2D image of RF power distribution and they clearly demonstrated to the electrical circuit model of proposed design [35].

In this study, MTM based absorber which is also known as energy harvester, microwave image detector and 2×2 patch array antenna are proposed both harvesting and imaging applications. Absorbed energy by each cell is converted to the DC signal by using Schottky diodes and obtained DC signals are transferred to MATLAB environment to create the image of absorbed power. Observed signals are scaled to 256 grey levels to have clear images. Additionally, 2×2 array patch antenna and 8×8 energy harvester are fabricated and experimental measurements are obtained to verify the accuracy of the proposed imaging system. Absorption characteristics of the proposed energy harvester are examined with both numerical and experimental measurements and the results are compared each other. In addition, imaging tests are conducted by harvester structure with fabricated array antenna. Also, subwavelength imaging experiment is successfully carried out by using a professional yagi uda antenna.

2. Theory and design

Design, characterization and fabrication of MTM energy harvester based subwavelength imaging structure is investigated in this paper. MTM based microwave energy harvester and 2×2 microstrip patch antenna array are designed and operated at the frequencies between 5.42 GHz to 5.53 GHz to test as a microwave imaging device. The unit cell of the proposed energy harvester is illustrated in Fig. 1, and dimension parameters are given in Table 1. The unit cell is designed with the copper (thickness of 0.035 mm and conductivity 5.8×107 S/m) as resonator layer and FR-4 dielectric (thickness $t = 1.6$ mm, permittivity $\varepsilon = 4.3$ and loss tangent $tan\delta = 0.025$) as substrate layer and also back side of the structure is covered by copper plate to prevent transmitted signals. The mentioned dimensions and structure is chosen due to easily accessibility and appropriateness with the fabrication facilities. As shown in Fig. 1, the gap is adjusted as 4 mm between resonators to obtain high signal absorption. The mentioned efficient dimensions are evaluated by using parametric analysis and genetic algorithm approach to provide decided frequency response.

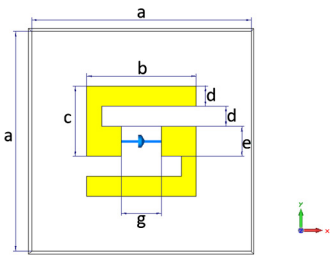

Fig. 1. The unit cell of the proposed MTM based absorber.

Table 1
Dimension parameters of harvester unit cell.

a	b	c	d	e	g
22 mm	11 mm	7 mm	2 mm	3 mm	4 mm

Numerical studies are carried out by using CST Studio Suite microwave simulator which is based on Finite Integration Technique (FIT). Moreover, the absorption can be calculated by the formula $A(w) = 1 - R(w) - T(w)$, where $R(w)$ corresponds reflection and $T(w)$ is transmission, also reflection and transmission can be obtained by using scattering parameters where $R(w) = |S_{11}|^2$ and $T(w) = |S_{21}|^2$. As mentioned before, back side of the designed harvester is covered by copper plate to prevent transmission, so transmitted energy can be ignored as $T(w) = 0$, thus absorption equations rearranged as $A(w) = 1 - R(w) = 1 - |S_{11}|^2$. This means that minimum reflection rises to maximum absorption so-called the maximum harvested energy.

3. Numerical study of harvester with array antenna

Numerical studies are achieved by using a commercial full wave EM solver FIT based microwave simulator. The boundaries are adjusted as electric field component $E = 0$ in x directions, magnetic field component $H = 0$ in y directions and open-space in z directions as shown in Fig. 2.a. This type of design provides Transverse Electromagnetic (TEM) incident microwave towards resonator side of proposed MTM structure. Also, 20 ohm resistive load is integrated on the gap of resonator layer to increase the signal absorption level which is also determined by parametric studies. This resistive load also collects electromagnetic energy and a Schottky diode is serially connected to resistive load on the gap between resonators to convert RF signal to DC signal. As given in Fig. 2.b, the proposed structure has significant signal absorption characteristic between the frequencies of 5.42 GHz to 5.53 GHz, and the absorption level has maximum value at the frequency of 5.48 GHz with a nearly perfect absorption value of 99.98%.

Moreover, electric field distribution is obtained and given in Fig. 3.a for maximum absorption. Electric field is mostly observed on the edges of the resonators and around the gap side. The concentrated electric field excites free electrons to cause surface currents as given in Fig. 3.b. These surface currents induce a voltage difference between resonator layers and can be collected by resistive lumped element. The incident microwave is an AC signal. Hence, it induces an AC RF voltage signal and it is converted to DC signal by the serially connected Schottky diode for the energy harvesting applications. Therefore, obtained DC voltage signal is used to represent a pixel value of each unit cells for subwavelength imaging.

Furthermore, a 2×2 microstrip patch array antenna is designed for high radiation properties in the frequencies range of 5.42 GHz and 5.53 GHz. The design of this specific antenna is due to high gain characteristic at the related frequency. The front view of the designed 2×2 array antenna is shown in Fig. 4 and dimension parameters are also given in Table 2. The designed antenna is an

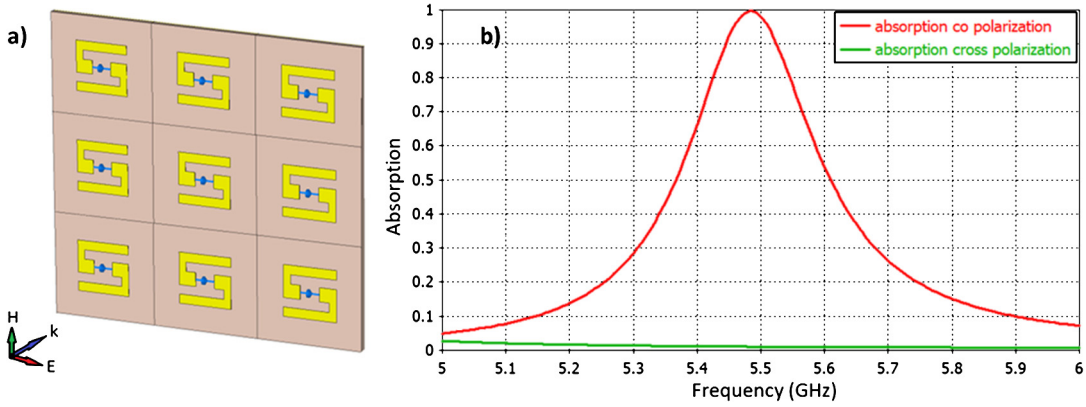

Fig. 2. a) Simulation set up of absorber structure, b) Absorption characteristics of proposed MTM structure.

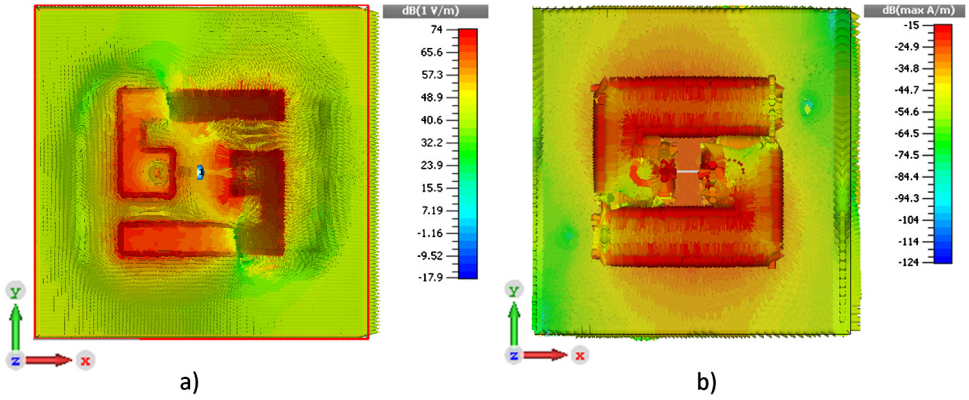

Fig. 3. a) Electric field, b) Surface current distributions of MTM based absorber cell.

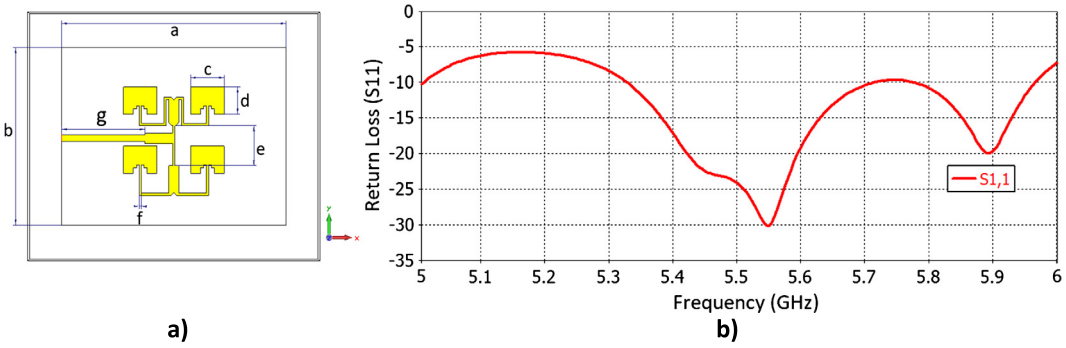

Fig. 4. a) Patch array antenna, b) Return loss of designed array antenna.

Table 2
Dimension parameters of 2×2 array antenna.

a	b	c	d	e	g
113 mm	84 mm	16.9 mm	12.85 mm	19 mm	42 mm

array antenna due to its advantages, such as high gain, directivity, wide band and low angular width.

In addition, specifically designed 2×2 array antenna for related frequency range illustrated in Fig. 5 which is also numerically analyzed by FIT based microwave simulator. It is also compared with a patch antenna operating at the same frequency. Discrete port having 50 ohm line impedance is connected to feed the antenna. The return loss (S_{11}) of designed antenna is examined to observe operation efficiency as shown in Fig. 4.b. There is a minimum return loss value at 5.52 GHz with a wideband operation range between 5.35 GHz and 5.65 GHz. The radiation pattern of single patch antenna and 2×2 array antenna are obtained and given in Fig. 5 at the frequency of 5.456 GHz which corresponds frequency range of the energy harvester structure. Fig. 6.a shows that single microstrip patch antenna has lower main lobe magnitude and directivity, therefore 2×2 array patch antenna is designed and operated as given in Fig. 5.b. According to radiation pattern of array antenna, its angular width is 43.2° and main lobe magnitude is 11.8 dBi. Whereas the side lobe level and angular width is reduced, main lobe magnitude of 2×2 array patch antenna is significantly improved with respect to singular patch antenna. Hence, this design can prove better observation of imaging for each unit cell on the harvester array.

4. Experimental study of harvesting and imaging

In this section, 8×8 MTM based energy harvester and 2×2 microstrip patch array antenna is fabricated and experimental studies

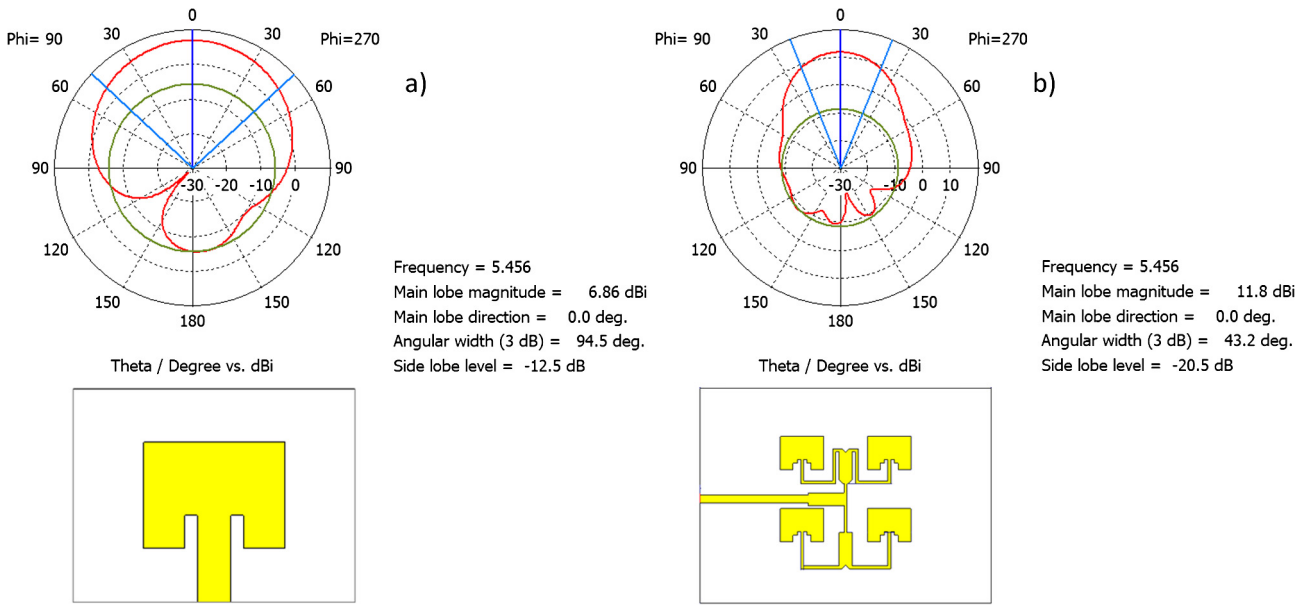

Fig. 5. Radiation pattern of designed a) single patch antenna, b) 2×2 array antenna.

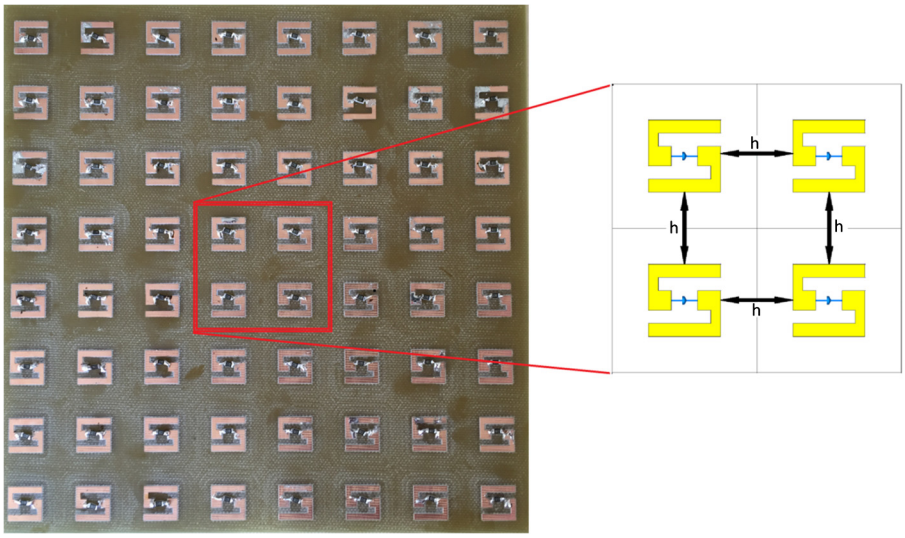

Fig. 6. Fabricated Sample-Distance between near unit cells represented by $h = 11$ mm.

are carried out. Operation frequency is set to 5.456 GHz in the experimental measurements. Designed MTM based absorber, called as energy harvester, is a subwavelength structure due to its dimensions with respect to the wavelength. Each cell has 22 mm of edge length and wavelength of incident microwave is 54.89 mm, thus proposed absorber is a type of subwavelength structure.

CNC controlled LPKF-E33 Protomat is used in the fabrication process and fabricated structure is given in Fig. 6 with a 11 mm distance between each unit cells ($h = 11$). According to Fig. 6, distance 'h' is obtained by using optimization techniques and its maximum value reduces the mutual interaction between cells to minimum. Accordingly, mutual effects caused by nearest cells are minimized with the edge dimensions of 22 mm and the distance between nearest cells of 11 mm. "h" is 5 times smaller than its wavelength ($f = 5.5$ GHz, $\lambda = 55$ mm) and this configuration shows designed structure is an subwavelength structure. Also, these interactions must be minimized, since each cell represents a pixel value with 256 grey levels under incident electromagnetic wave in microwave imaging application.

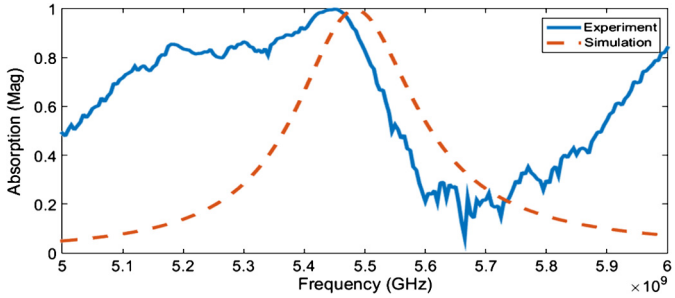

Fig. 7. Experimental and simulation results of absorber structure.

In the experimental phase, at first, Rohde Schwartz ZVL vector network analyzer and a wide band horn antenna are used to obtain reflection (S11) of designed absorber-harvester and obtained results are compared with simulation as shown in Fig. 7. The maximum absorption is observed at 5.48 GHz in the simulation program, which is in a good agreement with experimental study (5.45 GHz). Small frequency shift and noises observed are

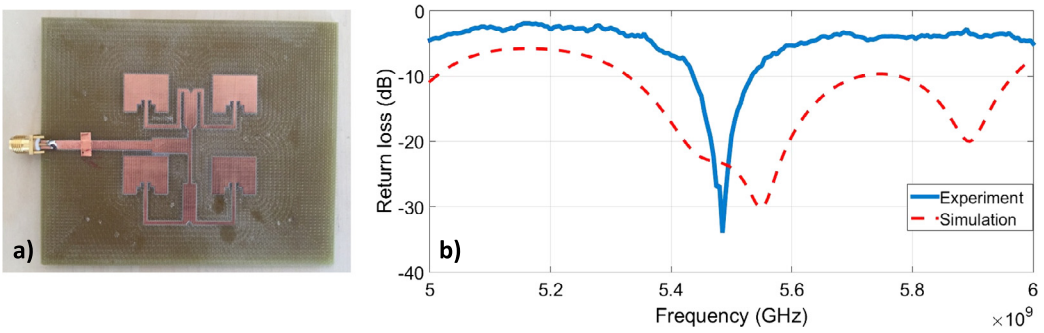

Fig. 8. a) Fabricated 2×2 array antenna after tuning, b) Experimental and simulation results of array antenna.

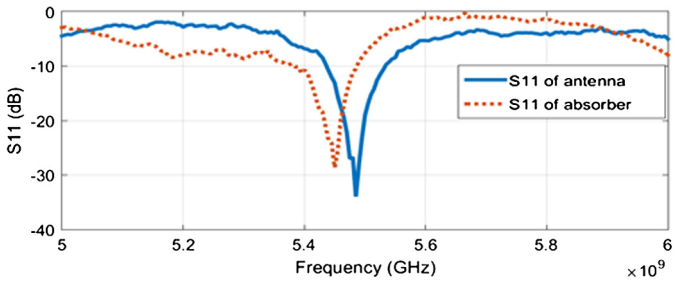

Fig. 9. Experimental results of fabricated antenna and absorber structure.

due to imperfection of experimental environment and manufacturing defects. Main reason about distinction between simulation and experiment is fabrication imperfection such as fabrication device faults, soldering faults and laboratory conditions. Even so, fabricated structure has a good absorption around unity between 5.4 GHz and 5.48 GHz. In addition, a 2×2 array patch antenna is also fabricated (Fig. 8.a) and tested with a vector network analyzer and obtained return losses (S11) are illustrated in Fig. 8.b. After fabrication process, antenna is tuned with a metal strip to have resonance frequencies between 5.4 GHz and 5.5 GHz as shown in Fig. 8.b. As given in Fig. 8.b., measured and simulated results are in the same band, whereas fabricated antenna has narrow band in experimental measurement. Therefore, the most important part as the agreement between fabricated array antenna and absorber-harvester structure frequency band is achieved. Fabricated absorber and array antenna can be operated between the frequencies of 5.4 GHz – 5.5 GHz and 5.43 GHz – 5.58 GHz, respectively. As a result, both fabricated antenna and absorber can be operated in the frequencies between 5.43 GHz and 5.5 GHz, as illustrated in Fig. 9. Also, the maximum power transfer occurs at the frequency of 5.456 GHz.

Incident electromagnetic wave is a form of the AC signal which should be converted to DC voltage to observe induced energy on the lumped element. Hence, a BAS4-05 general purposed Schottky diode and a 20 ohm resistive load are located serially on the gap between the resonator layers to convert AC signal to DC voltage which process is similar to one given in [33]. Observed DC signal on diode is transferred to MatLab environment via a microcontroller board and obtained voltage signals represented by 256 grey levelled pixels in MatLab. In the imaging part of this study, MAN&TEL MATS-100 antenna trainer is used for the frequencies between 5 GHz and 6 GHz to transfer adjustable microwave power. This antenna trainer has maximum operation power of 5 dBm and fabricated array antenna is operated at 5.456 GHz frequency. As illustrated in Fig. 10, 4.2 mV DC voltage difference is observed under incident electromagnetic energy with the distance of 20 cm, and the maximum voltage difference is observed with the distance of 1 cm as 13.5 mV.

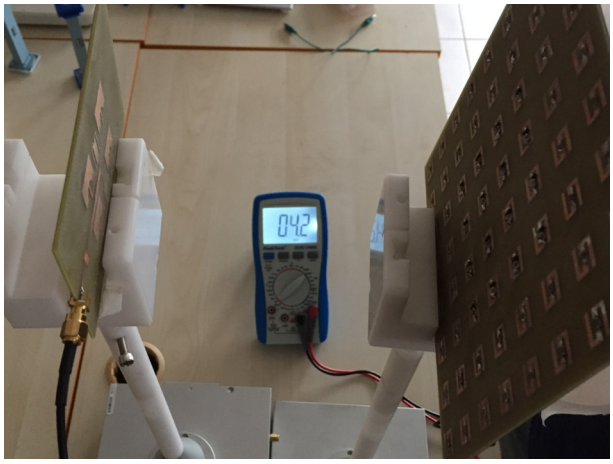

Fig. 10. Energy harvesting experiment.

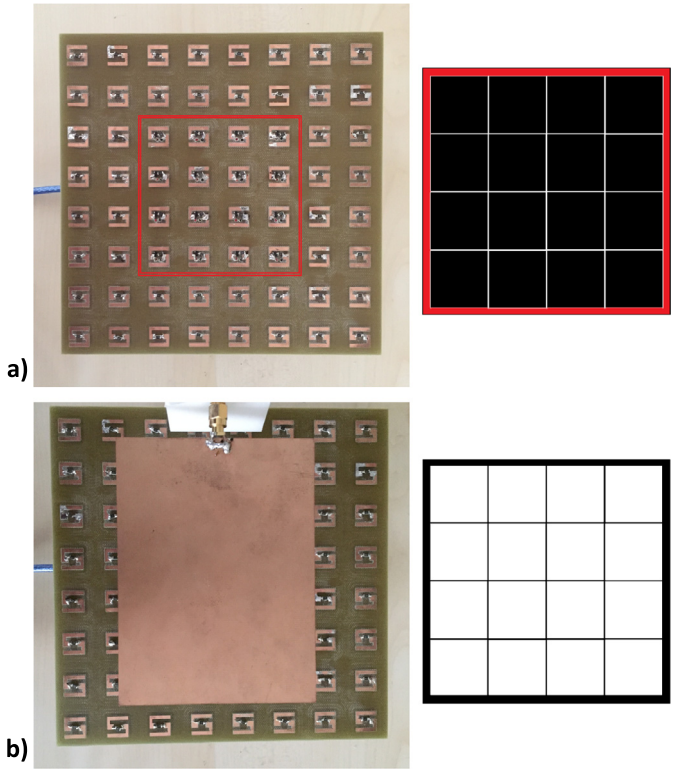

Fig. 11. a) Observed 4×4 image without antenna, b) Observed image under EM wave.

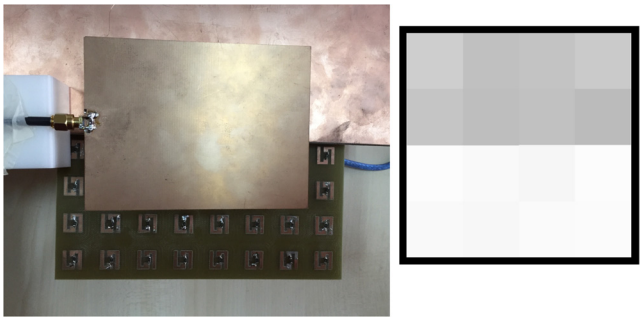

Fig. 12. Observed image with metal plate.

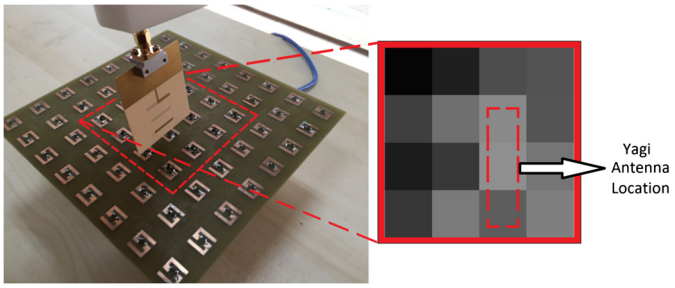

Fig. 13. Subwavelength imaging, antenna is located on the a33 cell.

In the imaging part of this study, MATLAB is used to monitor the grey pixelled view of the incident signals. Centered 4×4 cells are represented by 4×4 pixels with 0–255 grey levels scaled by 0–13.5 mV DC voltage signals. As in Fig. 11.a., there is no voltage difference between the resonator layers without any incident EM signal and each pixel are represented by the black colour. Another study is carried out under incident EM wave via 2×2 array patch antenna and results having 4×4 pixels with the distance of 4 cm are given in Fig. 11.b. In this circumstance, EM waves causes surface currents and DC voltage differences. Those voltage differences are observed on the gap of each cell and represented by 4×4 white coloured pixels.

Afterwards, a metal plate is located between the antenna and harvester layer to see the effects of metal plate on imaging process of EM wave and mutual interaction between cells. Experimental set up model is illustrated in Fig. 12, metallic plate has partially prevented incident EM signals and some incident signals are transformed to surface currents on the plate. Hence, the metallic plate can behave as antenna to radiate signals to absorber layer. So, first 2×4 pixels are shown in grey colours and second 2×4 pixels are shown nearly white because of there is no metal in front of them to block EM signals.

Final experiment is carried out with professional Yagi Uda antenna for subwavelength imaging application. Yagi Uda antenna is vertically located on the 4×4 structure and observed image is experimentally given in Fig. 13. Yagi Uda antenna is radiated directionally into the harvester structure and radiated waves are absorbed by each cell and converted to pixel values. Observed 4×4 image shows the location of Yagi Uda antenna with grey levels as given in Fig. 13. It can be concluded that the proposed structure is highly location sensitive and the mutual interaction is low. This is demonstrated and provided by using both Yagi Uda antenna and 2×2 array antenna.

5. Conclusions

In this work, we investigated to find out the feasibility of subwavelength image detection of incident EM wave by MTM based energy harvester both numerically and experimentally. Designed unit cell of MTM based energy harvester is examined and it has very high absorption phenomena at 5.456 GHz, which can be used in WIMAX communication band. A 2×2 array patch antenna is also designed to apply high power incident EM waves toward energy harvester. Designed energy harvester and 2×2 array patch antenna are fabricated and various experiments are carried out. Fabricated energy harvester structure is 8×8 and maximum harvested DC voltage is obtained as 13.5 mV by each cell, so totally $8\times8\times13.5 = 864$ mV DC voltage can be harvested. In the imaging part of this study, 4×4 cells are chosen and induced DC voltage of 4×4 cells are transferred to Matlab environment, therefore 4×4 image is obtained from induced voltages. In addition, imaging experiments are carried out by fabricated 2×2 array antenna and professional Yagi Uda antenna. In addition, proposed structure with high imaging characteristic and low mutual interaction between close unit cells can be used in various areas such as energy harvesting, incident wave tracing, crack detection, spy device detection and medical imaging.

References

[1] V.G. Veselago, The electrodynamics of substances with simultaneously negative values of and μ, Sov. Phys. Usp. 10 (4) (1968) 509.
[2] D.R. Smith, W.J. Padilla, D.C. Vier, S.C. Nemat-Nasser, S. Schultz, Composite medium with simultaneously negative permeability and permittivity, Phys. Rev. Lett. 84 (18) (2000) 4184.
[3] R.A. Shelby, D.R. Smith, S. Schultz, Experimental verification of a negative index of refraction, Science 292 (5514) (2001) 77–79.
[4] D.R. Smith, J.B. Pendry, M.C. Wiltshire, Metamaterials and negative refractive index, Science 305 (5685) (2004) 788–792.
[5] D. Schurig, J.J. Mock, B.J. Justice, S.A. Cummer, J.B. Pendry, A.F. Starr, D.R. Smith, Metamaterial electromagnetic cloak at microwave frequencies, Science 314 (5801) (2006) 977–980.
[6] H. Chen, B.I. Wu, B. Zhang, J.A. Kong, Electromagnetic wave interactions with a metamaterial cloak, Phys. Rev. Lett. 99 (6) (2007) 063903.
[7] W. Cai, U.K. Chettiar, A.V. Kildishev, V.M. Shalaev, Optical cloaking with metamaterials, Nat. Photonics 1 (4) (2007) 224–227.
[8] O. Altintas, E. Unal, O. Akgol, M. Karaaslan, F. Karadag, C. Sabah, Design of a wide band metasurface as a linear to circular polarization converter, Mod. Phys. Lett. B 1750274 (2017).
[9] J. Zhu, G.V. Eleftheriades, Dual-band metamaterial-inspired small monopole antenna for WiFi applications, Electron. Lett. 45 (22) (2009) 1104–1106.
[10] A. Erentok, R.W. Ziolkowski, Metamaterial-inspired efficient electrically small antennas, IEEE Trans. Antennas Propag. 56 (3) (2008) 691–707.
[11] N. Fang, X. Zhang, Imaging properties of a metamaterial superlens, Appl. Phys. Lett. 82 (2) (2003) 161–163.
[12] K. Aydin, I. Bulu, E. Ozbay, Subwavelength resolution with a negative-index metamaterial superlens, Appl. Phys. Lett. 90 (25) (2007) 254102.
[13] O. Altintas, M. Aksoy, O. Akgol, E. Unal, M. Karaaslan, C. Sabah, Fluid, strain and rotation sensing applications by using metamaterial based sensor, J. Electrochem. Soc. 164 (12) (2017) B567–B573.
[14] Y.I. Abdulkarim, L. Deng, O. Altintas, E. Unal, M. Karaaslan, Metamaterial absorber sensor design by incorporating swastika shaped resonator to determination of the liquid chemicals depending on electrical characteristics, Physica E, Low-Dimens. Syst. Nanostruct. (2019) 113593.
[15] M. Bakır, Ş. Dalgaç, M. Karaaslan, F. Karadağ, O. Akgol, E. Unal, T. Depçi, C. Sabah, A comprehensive study on fuel adulteration sensing by using triple ring resonator type metamaterial, J. Electrochem. Soc. 166 (12) (2019) B1044–B1052.
[16] N. Zheng, M. Aghadjani, K. Song, P. Mazumder, Metamaterial sensor platforms for Terahertz DNA sensing, in: Nanotechnology (IEEE-NANO), 2013 13th IEEE Conference on, IEEE, August 2013, pp. 315–320.
[17] N.I. Landy, S. Sajuyigbe, J.J. Mock, D.R. Smith, W.J. Padilla, Perfect metamaterial absorber, Phys. Rev. Lett. 100 (20) (2008) 207402.
[18] F. Dincer, M. Karaaslan, C. Sabah, Design and analysis of perfect metamaterial absorber in GHz and THz frequencies, J. Electromagn. Waves Appl. 29 (18) (2015) 2492–2500.
[19] M. Li, H.L. Yang, X.W. Hou, Y. Tian, D.Y. Hou, Perfect metamaterial absorber with dual bands, Prog. Electromagn. Res. 108 (2010) 37–49.
[20] Y. Ma, Q. Chen, J. Grant, S.C. Saha, A. Khalid, D.R. Cumming, A terahertz polarization insensitive dual band metamaterial absorber, Opt. Lett. 36 (6) (2011) 945–947.
[21] C.M. Watts, X. Liu, W.J. Padilla, Metamaterial electromagnetic wave absorbers, Adv. Mater. 24 (23) (2012).
[22] O. Akgol, O. Altintas, E.E. Dalkılınc, E. Unal, M. Karaaslan, C. Sabah, Metamaterial absorber-based multisensor applications using a meander-line resonator, Opt. Eng. 56 (8) (2017) 087104.

[23] Y.Z. Cheng, C. Fang, Z. Zhang, B. Wang, J. Chen, R.Z. Gong, A compact and polarization-insensitive perfect metamaterial absorber for electromagnetic energy harvesting application, in: Progress in Electromagnetic Research Symposium (PIERS), IEEE, August 2016, pp. 1910–1914.
[24] K.K.A. Devi, N.C. Hau, C.K. Chakrabarty, N.M. Din, Design of patch antenna using metamaterial at GSM 1800 for RF energy scavenging, in: Wireless and Mobile, 2014 IEEE Asia Pacific Conference on, IEEE, August 2014.
[25] C. Mulazimoglu, E. Karakaya, S. Can, A.E. Yilmaz, B. Akaoglu, Hexagonal-shaped metamaterial energy harvester design, in: Advanced Electromagnetic Materials in Microwaves and Optics (METAMATERIALS), 2016 10th International Congress on, IEEE, September 2016, pp. 82–84.
[26] T.S. Almoneef, O.M. Ramahi, Harvesting electromagnetic energy using metamaterial particles, in: Antennas and Propagation Society International Symposium (APSURSI), 2013 IEEE, IEEE, 2013 July, pp. 1046–1047.
[27] M. Bağmancı, O. Akgöl, M. Özaktürk, M. Karaaslan, E. Ünal, M. Bakır, Polarization independent broadband metamaterial absorber for microwave applications, Int. J. RF Microw. Comput.-Aided Eng. 29 (1) (2019) e21630.
[28] X. Duan, X. Chen, L. Zhou, A metamaterial harvester with integrated rectifying functionality, in: Wireless Information Technology and Systems (ICWITS) and Applied Computational Electromagnetics (ACES), 2016 IEEE/ACES International Conference on, IEEE, March 2016, pp. 1–2.
[29] M. Bağmancı, M. Karaaslan, E. Unal, M. Özaktürk, O. Akgol, F. Karadağ, A. Bhadauria, M. Bakır, Wide band fractal-based perfect energy absorber and power harvester, Int. J. RF Microw. Comput.-Aided Eng. 29 (7) (2019) e21597.
[30] B. Mulla, C. Sabah, Multiband metamaterial absorber design based on plasmonic resonances for solar energy harvesting, Plasmonics 11 (5) (2016) 1313–1321.
[31] M. Karaaslan, M. Bağmancı, E. Ünal, O. Akgol, C. Sabah, Microwave energy harvesting based on metamaterial absorbers with multi-layered square split rings for wireless communications, Opt. Commun. 392 (2017) 31–38.
[32] B. Wood, J.B. Pendry, D.P. Tsai, Directed subwavelength imaging using a layered metal-dielectric system, Phys. Rev. B 74 (11) (2006) 115116.
[33] Y. Xie, X. Fan, Y. Chen, J.D. Wilson, R.N. Simons, J.Q. Xiao, A subwavelength resolution microwave/6.3 GHz camera based on a metamaterial absorber, Sci. Rep. 7 (2017).
[34] F.O. Alkurt, O. Altintas, A. Atci, M. Bakir, E. Unal, O. Akgol, K. Delihacioglu, M. Karaaslan, C. Sabah, Antenna-based microwave absorber for imaging in the frequencies of 1.8, 2.45, and 5.8 GHz, Opt. Eng. 57 (11) (2018) 113102.
[35] S. Yagitani, K. Katsuda, M. Nojima, Y. Yoshimura, H. Sugiura, Imaging radio-frequency power distributions by an EBG absorber, IEICE Trans. Commun. 94 (8) (2011) 2306–2315.